IntraVital 3, e28770; April 2014; © 2014 Landes Bioscience

Clinical applications of optical coherence tomography in urology

Hsing-Wen Wang and Yu Chen*

Fischell Department of Bioengineering; University of Maryland; College Park, MD USA

Keywords: optical coherence tomography, doppler optical coherence tomography, bladder, kidney, ureter

Abbreviations: OCT, optical coherence tomography; SS-OCT, swept source/OCT; OFDI, optical frequency domain imaging; DOCT, doppler optical coherence tomography; UHR, ultrahigh-resolution; TCC, transitional-cell carcinoma; CIS, carcinoma in situ; HFUS, high-frequency ultrasound

Since optical coherence tomography (OCT) was first demonstrated in 1991, it has advanced significantly in technical aspects such as imaging speed and resolution, and has been clinically demonstrated in a diverse set of medical and surgical applications, including ophthalmology, cardiology, gastroenterology, dermatology, oncology, among others. This work reviews current clinical applications in urology, particularly in bladder, urether, and kidney. Clinical applications in bladder and urether mainly focus on cancer detection and staging based on tissue morphology, image contrast, and OCT backscattering. The application in kidney includes kidney cancer detection based on OCT backscattering attenuation and non-destructive evaluation of transplant kidney viability or acute tubular necrosis based on both tissue morphology from OCT images and function from Doppler OCT (DOCT) images. OCT holds the promise to positively impact the future clinical practices in urology.

Principle and Instrumentation of OCT

OCT is an emerging medical imaging technology which enables cross-sectional imaging of tissue microstructure in situ and in real-time.[1] OCT can achieve 1–10 μm resolutions and 1–2 mm penetration depths, approaching those of standard excisional biopsy and histopathology, but without the need to remove and process tissue specimens.[2] OCT is analogous to ultrasound imaging, except that imaging is performed by measuring the echo time delay and intensity of backscattered light rather than sound. OCT imaging can be performed fiber-optically using delivery devices such as hand-held probes, endoscopes, catheters, laparoscopes, and needles which enable non-invasive or minimally-invasive internal body imaging.[3,4]

Figure 1A shows a schematic of time-domain OCT. Measurements are performed using a Michelson interferometer with a low coherence length (broadband) light source. One arm of the interferometer illuminates the light on the tissue and collects the backscattered light (typically referred to as "sample arm"). Another arm of the interferometer has a reference path delay which is scanned as a function of time (typically referred to as "reference arm"). Optical interference between the light from the sample and reference arms occurs only when the optical delays match to within the coherence length of the light source.

Alternatively, OCT interference signals can be detected in frequency or Fourier domain. In Fourier-domain OCT, the reference mirror position is fixed, and echoes of light are obtained by Fourier transforming the interference spectrum. These techniques are somewhat analogous to Fourier transform spectroscopy and have a significant sensitivity and speed advantage compared with time-domain OCT because they measure the optical echo signals from different depths along the entire axial scan simultaneously rather than sequentially. Fourier-domain detection enables 10–100 folds improvement in detection sensitivity and speed over the time-domain configuration.[5-7] These advances greatly improve the performance of OCT, enabling three-dimensional OCT (3D-OCT) imaging in vivo.

Fourier-domain OCT can be performed using two complementary techniques, known as spectral/Fourier-domain OCT and swept-source/Fourier-domain OCT (SS-OCT, also known as Optical Frequency Domain Imaging, OFDI). Spectral/Fourier-domain detection uses a spectrometer and a high speed line scan camera to measure the interference spectrum in parallel (see **Fig. 1B**).[8,9] In contrast, swept-source/Fourier-domain OCT uses a frequency-swept laser light source and a photodetector to measure the interference spectrum (see **Fig. 1C**).[10-12] Three-dimensional imaging of biological tissue in vivo enabled by Fourier-domain OCT promises to have a powerful impact in disease diagnosis[13,14] and therapy monitoring.[15,16] Up to date, many clinical applications using OCT have demonstrated in a diverse set of medical and surgical specialties. Several commercially-available devices have received US Food and Drug Administration (FDA) clearance to be sold in the market,[17] such as Imalux Corporation (**Fig. 1D**) whose OCT system is based on time-domain mechanism for endoscopic imaging, and LightLab Imaging (now part of St. Jude Medical, Inc.) (**Fig. 1E**) that adapts frequency-domain mechanism for their OCT system in cardiovascular imaging.

*Correspondence to: Yu Chen; Email: yuchen@umd.edu
Submitted: 02/07/2014; Revised: 04/01/2014; Accepted: 04/03/2014;
Published Online: 04/30/2014; http://dx.doi.org/10.4161/intv.28770

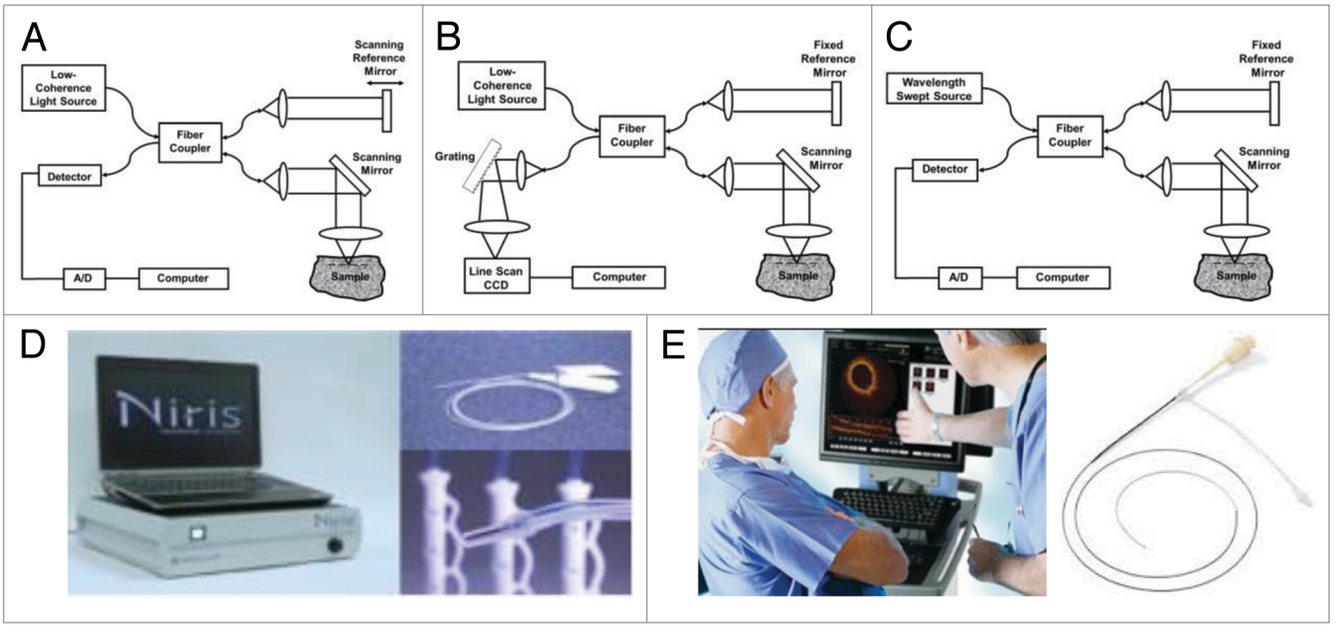

Figure 1. Schematics of (**A**) time-domain, (**B**) spectral / Fourier-domain, and (**C**) swept-source / Fourier-domain OCT systems. (**D**) A Clinical OCT system and endoscopic probes from Imalux Corporation. (**E**) A clinical vascular OCT system and the fiber optic probe from LightLab Imaging (now St. Jude Medical, Inc.).

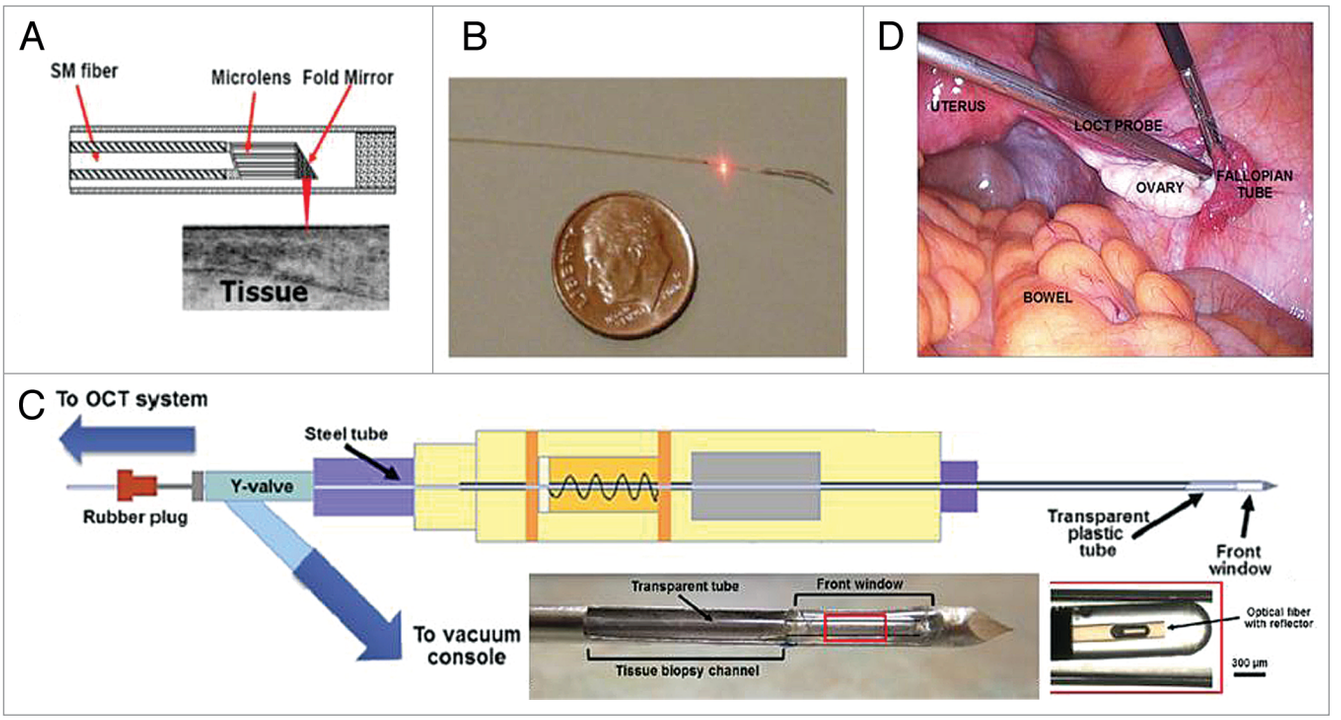

Figure 2. Fiber-optic probes for catheter/endoscope, biopsy needle, and laparoscope. (**A**) Schematic of the distal end of an OCT probe. (**B**) Photograph of an intravascular imaging catheter (0.4 mm in diameter). (**C**) Schematic of a modified core-needle biopsy device with a catheter-based OCT probe (figures are adapted from reference[25] with permission) and photographs of modified tip. (**D**) The photograph of a custom laparoscopic OCT probe for imaging human ovary. Figures are adapted from reference 21 with permission.

To image internal organs, miniaturized catheter/endoscope imaging devices have been developed for intraluminal and intravascular imaging.[18,19] Other imaging devices such as laparoscopes[20,21] and needle imaging device have been developed to enable solid organ imaging.[22-27] Nowadays, various OCT imaging probes have been developed for different clinical

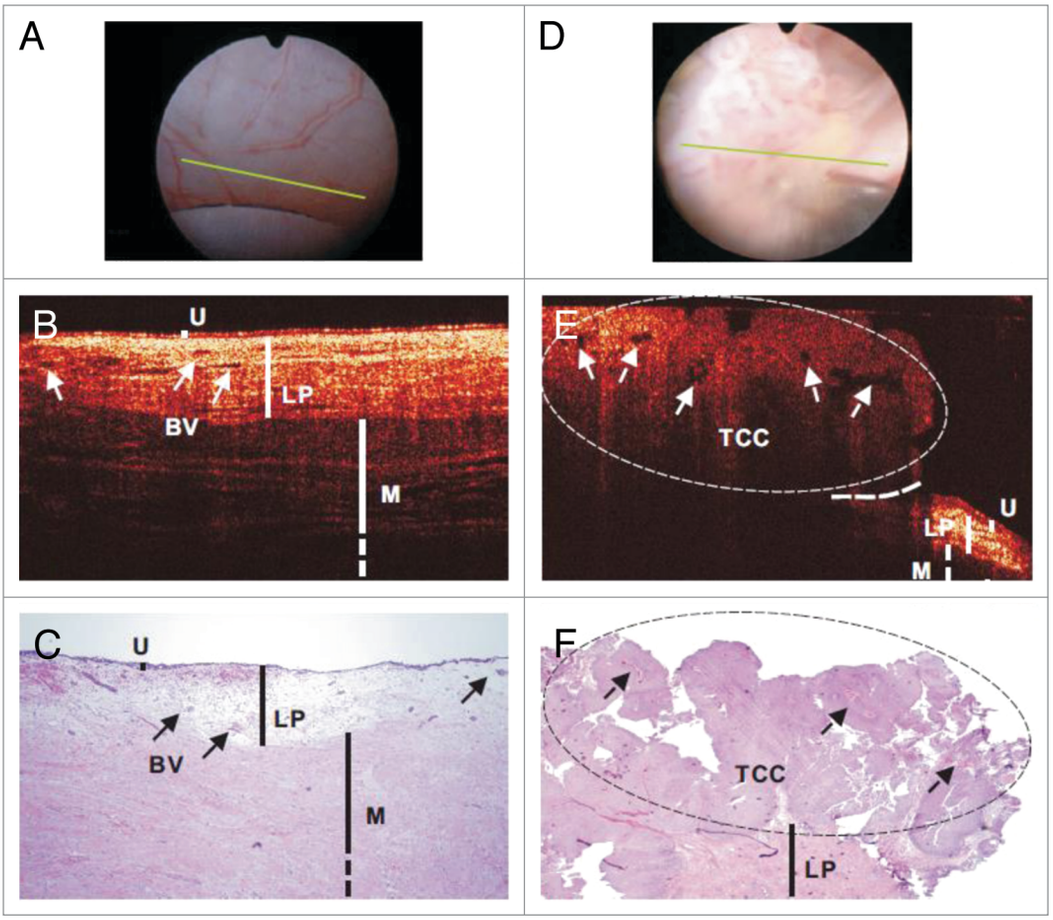

Figure 3. In vivo surface (**A** and **D**), cross-sectional OCT (**B** and **E**), and H&E-stained histologic images (**C** and **F**) of normal human bladder (**A–C**) vs a papillary TCC (**D–F**). The morphologic details of normal bladder (U, urothelium; LP, lamina propria; M, upper muscularis) were clearly delineated by OCT, but those of papillary TCC diminished. Solid arrows: subsurface blood vessels; dashed arrows: papillary features; dashed circle: TCC, identified by OCT based on increased urothelial heterogeneity; dashed line: boundary with adjacent normal bladder. Figures and captions are adapted from reference 107 with permission.

applications.[23,28-43] Development of such devices facilitates the translation of OCT to clinical applications and allows clinicians to use the enhanced imaging capabilities of this technique to benefit the patients.

Figure 2A shows the schematic of a representative OCT catheter/endoscope device consisting of a hollow cable carrying a single-mode (SM) optical fiber. The beam from the distal end of the fiber is focused by a gradient-index (GRIN) microlens and is directed perpendicular to the catheter axis by a microprism or micromirror. The distal optics is encased in a transparent housing. The beam can be scanned either circumferentially (by rotating the cable) or linearly (by translating the cable) to form a cross-sectional OCT image. The outer diameter of the catheter/endoscope can be made small enough to image inside a human coronary artery (see **Figure 2B**). **Figure 2C** shows the schematic of a catheter based OCT (from St. Jude Medical, Inc.) combined with a modified vacuum-pumped biopsy needle.[25] This modified core-needle biopsy device includes the addition of a transparent front window for real-time OCT guidance, the addition of a long steel/plastic tube through which the OCT catheter is inserted, and a Y-valve to allow both linear access for the OCT catheter and the vacuum/pressure tube connection. **Figure 2D** depicts a custom laparoscopic OCT device imaging the ovaries in patients undergoing oophorectomy.[21]

Clinical Applications of OCT

Since its invention in 1991, OCT has rapidly developed as a non-invasive biomedical imaging modality that enables cross-sectional visualization of tissue microstructures in vivo.[44-47] The resolution of OCT is one to two orders of magnitude higher than conventional ultrasound, approaching that of histopathology, thereby allowing architectural morphology to be visualized in situ and in real-time. OCT enables imaging of structures in which biopsy would be hazardous or impossible, and promise to reduce the sampling errors associated with excisional biopsy. OCT has been translated from bench to various clinical applications including ophthalmology,[48] cardiology,[49-52] gastroenterology,[28,53-67] dermatology,[68-70] dentistry,[71-73] urology,[74-77] gynecology,[78-80]

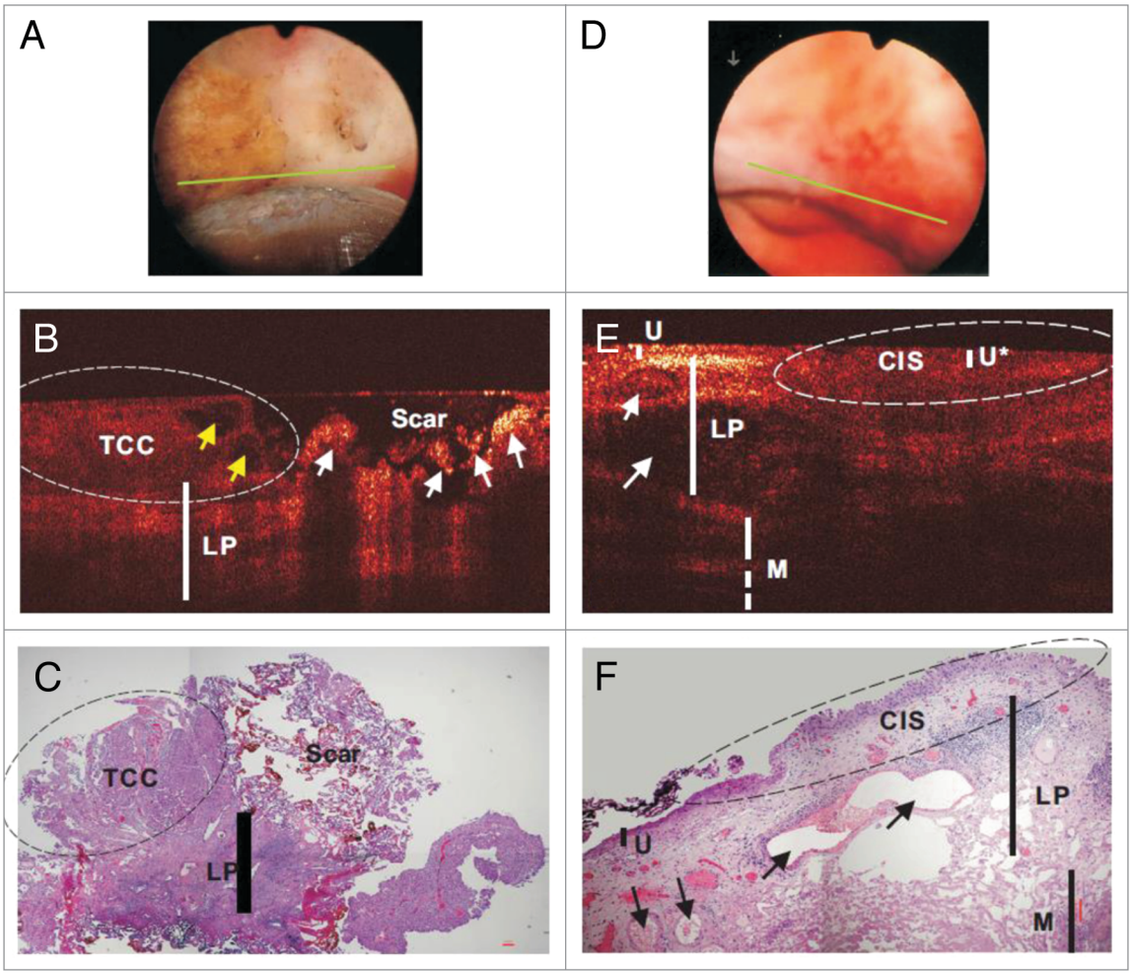

Figure 4. In vivo surface (**A** and **D**), cross-sectional OCT (**B** and **E**), and H&E-stained histologic images (**C** and **F**) of a recurrent TCC post-TUR bladder tumor (**A–C**) and a CIS (**D–F**). Yellow and white arrows: papillary features and scar or necrotic lesions. OCT differentiation of TCC (left circle) vs scar was based on low-scattering and papillary features in TCC vs ultrahigh superficial scattering with abruptly diminished underlying architecture in scar or necrotic lesion, which was nonspecific under surface image (**A**). Arrows in (**E** and **F**): blood vessels. The morphology (e.g., lamina propria [LP] and muscularis [M]) under CIS (U*) diminished. CIS was low backscattering and identified by OCT based on increased urothelial heterogeneity and less distinguishable U-LP interface. Figures and captions are adapted from reference 107 with permission.

among others.[52] The most developed clinical OCT applications are those focusing on ophthalmic, cardiovascular, and oncologic imaging. For the application in oncology, many cancers arise from the epithelial layers, and demonstrate disruption of normal architectural morphology of tissues. The resolution and imaging field-of-view of OCT is approaching those of standard biopsy and histopathology, therefore OCT represents a potential method for "optical biopsy" of the tissue in situ, which can guide the excision biopsy to improve the sampling accuracy. OCT has shown promises in detecting structural alterations associated with malignancies including those arising in the breast,[81-85] bladder,[77,86-89] brain,[90-92] gastrointestinal,[65,66,93,94] respiratory[95] and reproductive tracts,[96,97] skin,[98] larynx,[99,100] and oral cavity.[101,102]

Clinical applications of OCT in ophthalmology,[48,52] cardiology,[52,103] and gastroenterology[28,53-67] have been reviewed extensively elsewhere. In this review, we focus on clinical OCT applications in urology, particularly in bladder, ureter, and kidney.

Bladder

Bladder cancer originates in the urothelium and is curable if diagnosed and treated early, but has a high mortality rate in advanced stages.[104] However, early diagnosis of bladder cancer remains a clinical challenge. The other problem is its high recurrence rate resulting in lifelong follow-up and possible repeated treatments, which make bladder cancer one of the most expensive cancers to manage. Currently, white light cystoscopy (WLC) is the standard for initial bladder cancer diagnosis with several shortcomings such as flat carcinoma in situ (CIS) is difficult to visualize. OCT and several other optical imaging techniques (such as fluorescence imaging) have been developed to better identify and characterize bladder lesions beyond what is possible with standard WLC.

Over the last decade, both ex vivo[88,105,106] and in vivo studies[76,77,89,107-109] have been conducted on the ability of OCT to detect bladder cancer by resolving the changes of bladder wall

Table 1. Summary of OCT Patient Studies in diagnosis of urological diseases

Reference number	Number of Patients	Sensitivity(%), Specificity(%), and others	Determination of diseases by OCT	OCT image features
Bladder				
89	32	90, 89, 90(PPV), 89(NPV)[a] 75, 97, 75(PPV), 97(NPV) 100,90,70(PPV), 100 (NPV)	Tumor confined to the mucosa (Ta); Lamina propria-invasive tumor (T1); Muscle-invasive tumor (T2)	Enhanced urothelial heterogeneity and/or urothelial thickening
77	24	100, 89, 75 (PPV), 100 (NPV), 92 (accuracy) 90 (PPV)	Bladder carcinoma including 16 papillary Transitional-cell carcinoma (TCC) and 5 flat lesions; Tumor invasion	Enhanced urothelial heterogeneity and/or urothelial thickening
107	56	94, 81	CIS and TCC (Ta, T1, and T2)	TCC: enhanced urothelial heterogeneity and/or urothelial thickening; CIS: no obvious urothelial thickening, slightly decreased backscattering in urothelium, and drastically diminished backscattering in lamina propria layer
108	164 28	85, 68 100, 77	Bladder carcinoma; Differentiation between muscle-invasive and non-muscle-invasive TCC during TUR	Enhanced urothelial heterogeneity and/or urothelial thickening for carcinoma
106	142[b]	83.8, 78.1	Malignant bladder	Enhanced urothelial heterogeneity and/or urothelial thickening for carcinoma
Ureter				
134	8	Not available (NA)	Invasive tumor (pT1); Noninvasive tumor (pTa); CIS; Grade 2 vs. grade 3	Interruption of the basement membrane; Basement membrane appeared as a thin dark line below the tumor; Flat, broadened urothelial layer with low reflectivity without interruption of the basement membrane; Grade 3 lesions have higher calculated attenuation coefficient
Kidney				
135	16	NA	Malignant tumor	Malignant tumor has higher calculated attenuation coefficient than normal parenchyma
122	20	NA	Angiomyolipoma; Transitional cell carcinomas	Fat elements appear as lucent dark areas easily visible on OCT; Unique and layered papillary architecture
126	29	NA	Ischemic kidney	Close kidney parenchyma tubular, less blood flow from vessels and glomeruli

[a]PPV, positive predictive value; NPV, negative predictive value. [b]The number of fresh human bladder tissue samples.

layers in urothelium, lamina propria, and muscularis propria and/or the corresponding backscattering. A 32 patient study showed that OCT has high detection accuracy for real-time imaging and staging of bladder cancer adjunct to WLC (90% sensitivity and 89% specificity for tumor confined to the mucosa, and 100% sensitivity and 90% specificity for muscle-invasive tumors).[89] Another clinical study based on OCT imaging with 24 patients reported an overall sensitivity of 100%, specificity of 89%, and diagnostic accuracy of 92% for superficial bladder transitional-cell carcinoma (TCC).[77] A 56 patient study showed that the overall specificity of cystoscopic OCT (81%) was comparable to voided cytology (88.9%, $P = 0.49$), but significantly higher than WLC (62.5%, $P = 0.02$) in TCC diagnosis.[107] **Figure 3** illustrates in vivo WLC, OCT, and H&E images of normal human bladder (**Fig. 3A–C**) and TCC (**Fig. 3D–F**).[107] TCC exhibited enhanced urothelial heterogeneity as indicated by the arrows shown in **Figure 3E**. Furthermore, the same work also demonstrated better tumor margin detection using OCT to guide transurethral resection (TUR), which is commonly used for non-muscle-invasive bladder cancer such as TCC that attributes to approximately 75% of all bladder cancer,[110] and to enhance re-TUR cases where the scar or necrosis induced by previous TUR may make it difficult to identify residual or recurrent tumors by WLC. **Figure 4** shows in vivo WLC, OCT, and H&E images of TCC post-TUR (**Fig. 4A–C**) and carcinoma in situ (CIS) (**Fig. 4D–F**).[107] It demonstrated that OCT image

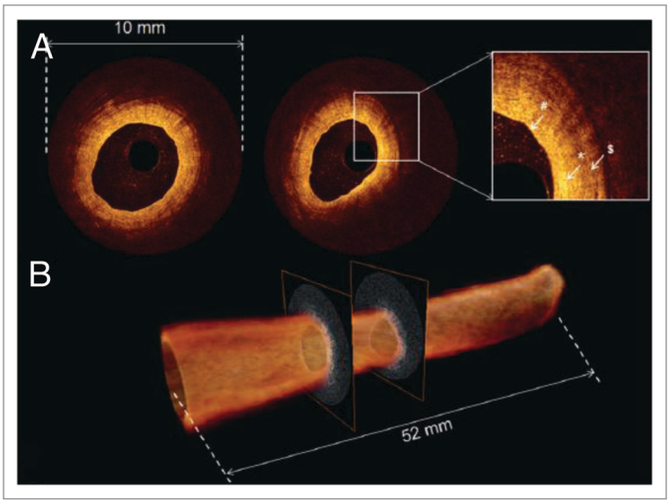

Figure 5. OCT of healthy ureter. (**A**) Individual OCT images obtained from volumetric OCT data set. Inset, higher magnification reveals normal ureter urothelium (pond sign), lamina propria (asterisk), and muscularis (dollar sign). (**B**) 520-frame volumetric data set across 52 mm trajectory along probe in approximately 5.2 s, resulting in 52 mm long by 10 mm diameter total scanned cylindrical volume. Figures and captions are adapted from reference 119 with permission.

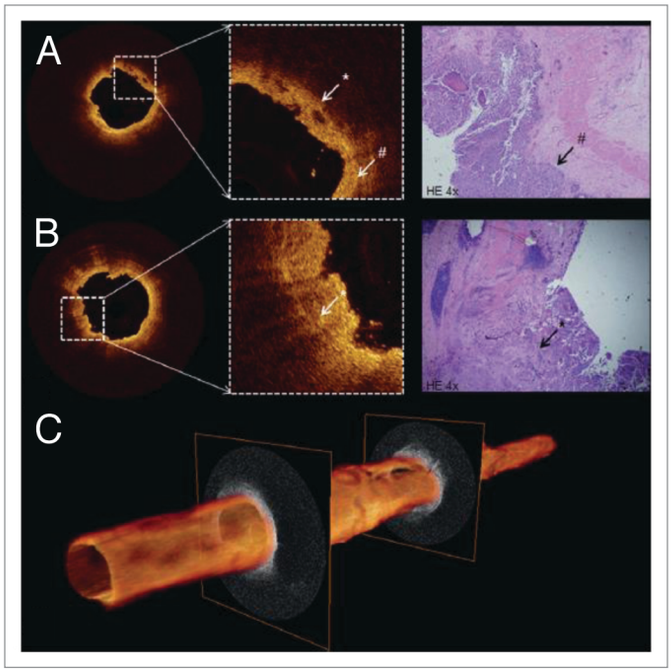

Figure 6. (**A** and **B**) Cross-sectional OCT images of proximal ureter show interruption (white asterisk) of thin dark line (white pound sign) suggesting invasive tumor. Distinction among anatomical layers was not possible. Corresponding histology reveled T3G3 urothelial carcinoma (black arrow). (**C**) 3D pullback of OCT built from 520 individual cross-sectional images over 5.2 cm length. Figures and captions are adapted from reference 119 with permission.

can differentiate recurrent TCC from scar or necrosis (**Fig. 4B**). CIS has low diagnostic sensitivity and specificity (e.g., 30–60%) under routine WLC and remains a critical clinical problem.[111,112] Its OCT image showed characteristics including no obvious urothelial thickening, slightly decreased backscattering in urothelium, and drastically diminished backscattering in lamina propria layer (**Fig. 4E**). Finally, Zagaynova et al. evaluated 28 cases with OCT during TUR to discriminate between muscle-invasive and non-muscle-invasive tumors with a sensitivity of 100% and specificity of 77%.[108] **Table 1** summarizes the performance of OCT in clinical diagnosis of urological diseases.

Computer-aided recognition of bladder cancer using OCT and texture analysis is under investigation to improve the clinical utility of OCT.[88] Higher OCT axial resolution demonstrated the ability to differentiate healthy urothelial tissue, CIS, and TCC from 142 fresh human bladder tissue samples.[106] The reported sensitivity and specificity to detect malignant bladder are 83.8% and 78.1%, respectively. Recently, real-time 3D-OCT imaging was demonstrated in 3 clinical cases with bladder/ureter carcinoma to show the contrast of muscle-invasive carcinoma area, the scar tissue area from normal bladder wall, and ureter with three distinguishable layers, including the urothelium, lamina propria, and muscularis layer.[113]

Similar to other techniques, OCT has some limitations in bladder cancer detection.[110,114] One is false-positives that may be induced by scarring[107] or inflammation of the mucosa.[89] More clinical studies are needed to confirm the reported results in detecting bladder cancer. The other limitation is the limited field-of-view (FOV) in both lateral and depth directions. OCT was compared with high-resolution ultrasound (i.e., 40 MHz high frequency ultrasound, HFUS) in a rat bladder cancer model.[87] Results showed that OCT could differentiate inflammatory lesions and TCC based on characterization of urothelial thickening and enhanced backscattering or heterogeneity, which HFUS failed due to insufficient image resolution and contrast. On the other hand, HFUS was able to stage large T2 tumors that OCT failed due to limited imaging depth. Multimodality cystoscopy combining OCT and HFUS, or the combination of OCT with larger lateral FOV technique such as WLC, narrow band imaging, and photodynamic diagnosis may help improve diagnosis and staging.[87,110,114,115]

Ureter

Few OCT studies have been conducted in ureter, which has somewhat similar mucosal morphology as bladder that the tissue surface is covered with urothelial cells. Early detection of ureteral cancer, as well as accurate tumor staging and grading, is also critical to reduce the mortality of the disease and help making the optimal treatment decisions.[116] The staging and grading of urothelial carcinoma in ureter is challenging because the narrow caliber makes biopsy difficult and unreliable. Endoscopic OCT (EOCT) is necessary to access the layer structures of the ureteral wall with sufficient resolution to stage early ureteral cancer. Several *ex-vivo* studies in porcine ureter have demonstrated to clearly distinguish anatomical layers particularly the urothelium and lamina propria layers[117,118] with better differentiation ability than endoluminal ultrasound.[117] Bus et al. reported the

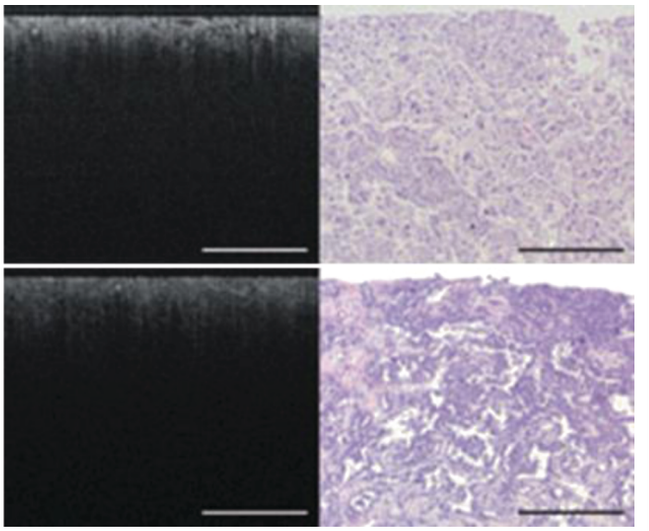

Figure 7. OCT image and corresponding light microscopy of renal carcinoma, chromophobe subtype (top panel) and papillary subtype, grade 4 (bottom panel). In the chromophobe subtype (top panel), collections of large polygonal cells arranged in trabeculae are seen as areas of intermediate brightness with intervening dark spaces on OCT. In the papillary subtype (bottom panel), elements of cuboidal cells surrounding a fibrovascular stalk were seen on light microscopy but not visible on the OCT image. Bars are 500 μm. Figures and captions are adapted from reference 122 with permission.

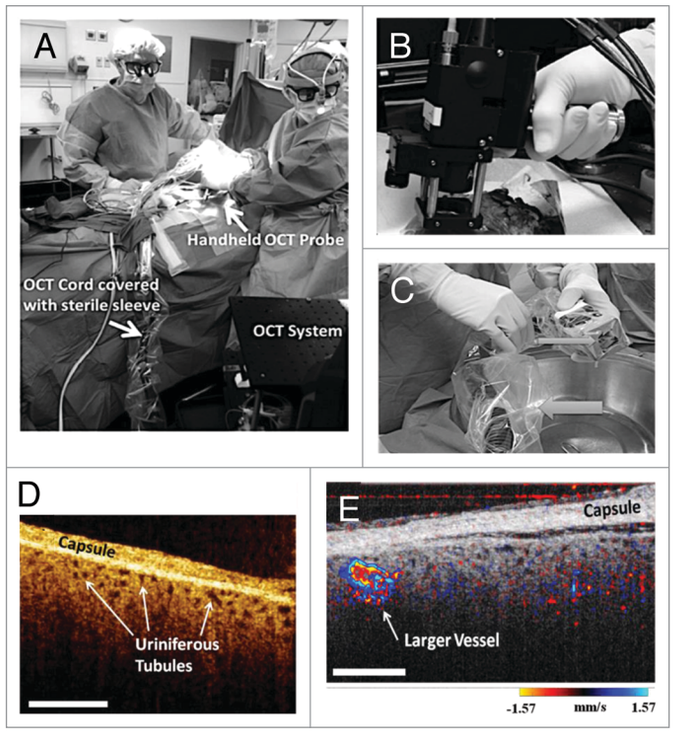

Figure 8. (**A**) Transplant surgeons used the sterilized hand-held OCT probe shown in (**B**) to image a transplanted human donor kidney in the operating room. Both surgeons are looking at real-time images of the functioning kidney. The OCT probe and associated wires are covered with a sterile camera sleeve. (**C**) The OCT imaging probe covered with transparent Tegaderm (small arrow). The cords leading to the probe are covered with a sterile camera sleeve (large arrow). (**D**) In vivo OCT imaging of human kidneys following transplantation showing open uriniferous tubules below the renal capsule. Tubules appear to be fairly open and round with some degree of homogeneity throughout the images. Scale bar is 500 μm. (**E**) In vivo human kidney showing open tubules and cortical blood flow. Open tubules appear round and relatively uniform across all images. Also, a larger blood vessel is seen. Scale bar is 500 μm. **D** and **E** are from reference 126 with permission.

intraluminal OCT identification of anatomical layers of the healthy human ureter in vivo and the results for grading and staging upper urinary track (UUT) urothelial carcinoma using OCT.[119] They identified several unique features by OCT although this study does not have enough patients to provide information on OCT's sensitivity and specificity of UUT diagnosis. Their study demonstrated that OCT can: (1) distinguish healthy tissues from tumors; (2) differentiate invasive and non-invasive tumors; (3) differentiate grade 2 and 3 lesions by quantifying OCT backscattering attenuation and, thus, has the potential to provide intraoperative real-time histological information on stage and grade during minimally-invasive procedures. **Figure 5** shows representative OCT images of healthy ureter with identified urothelium, lamina propria, and muscularis layers. **Figure 6** shows representative OCT images of invasive tumor (namely stage T3G3 urothelial carcinoma) where distinction among anatomical layers was not possible.

Kidney

OCT studies in clinical kidney diseases include applications in kidney cancer[120-122] and non-destructive evaluation of transplant kidney viability or acute tubular necrosis (ATN).[123-126] Barwari et al. conducted both an ex vivo study with 14 patients and an in vivo study with 16 cases. They demonstrated the capability of OCT to distinguish normal renal parenchyma from malignant renal tumors based on the backscattering properties. Both studies measured higher backscattering property in malignant tumors (measured from the surface or measured directly in the internal tumors) than normal parenchyma. The averaged backscattering value of three benign tumors reported in the in vivo study is between the value from normal and malignant tumor but it did not show significant difference from that of normal renal parenchyma and tumors. Linehan et al. imaged fresh surgical resected tissues of normal renal parenchyma and neoplasm using a laboratory OCT system with lateral resolution of 10 μm and axial resolution of 4 μm.[122] They found angiomyolipoma and transitional cell carcinomas[127,128] can be distinguished from normal parenchyma. However, higher resolution OCT is necessary to distinguish clear-cell tumors and other renal carcinoma subtypes from normal parenchyma and between carcinoma subtype themselves, which had a heterogeneous appearance on OCT. **Figure 7** shows OCT image and corresponding light microscopy of renal carcinoma, chromophobe subtype (top panel) and papillary subtype, grade

4 (bottom panel). Some defining features such as collections of large polygonal cells arranged in trabeculae in chromophobe renal carcinoma and elements of cuboidal cells surrounding a fibrovascular stalk in papillary renal carcinoma were not clearly evident on corresponding OCT images.

Acute tubular necrosis (ATN) is the most common insult to donor kidneys destined for transplantation.[129,130] ATN is caused by a lack of oxygen to the kidney (ischemia of the kidneys), and is one of the most common causes of kidney failure. Both ex vivo,[123-126] and in vivo[126] studies demonstrated the capability of OCT to visualize kidney parenchyma morphology and function (i.e., tubular morphology, blood flow from vessels and glomeruli) that provide information to kidney ischemic damage. **Figure 8** shows the hand-held OCT imaging device used in the operating room (**Fig. 8A–C**). **Figure 8D** depicts representative in vivo kidney OCT images after kidney transplant showing cross-sectional profiles of superficial proximal tubules below the renal capsules. The openness of tubule lumens labeled in **Figure 8D** reflects a functioning post-transplanted kidney. **Figure 8E** shows the combination of morphological imaging with OCT and functional imaging with DOCT for one patient that displayed good tubular morphology and blood flow. Fairly densely packed uriniferous tubules are observed with several cortical blood vessels indicating re-perfusion. Finally, **Video S1** shows combined OCT and DOCT real-time images of the living kidney following its transplant as would be seen while imaging the kidney in the operation room.

Summary

OCT is a powerful medical imaging technology that can reveal microstructure and blood flow in biological tissues in a non-invasive fashion and in real-time. Current technology improvements enable 3D-OCT imaging in real-time,[131-133] thereby dramatically reducing the motion artifacts during image acquisition when accurate quantification of OCT/DOCT image is essential for disease diagnosis and decision making. In addition, higher resolution might also help to enhance the classification of imaging parameters for disease diagnosis. With continued technology development and clinical translation, OCT promises to enhance current clinical practice in urology.

Disclosure of Potential Conflicts of Interest

No potential conflicts of interest were disclosed.

Supplemental Materials

Supplemental materials may be found here:
www.landesbioscience.com/journals/intravital/article/28770

References

1. Huang D, Swanson EA, Lin CP, Schuman JS, Stinson WG, Chang W, Hee MR, Flotte T, Gregory K, Puliafito CA, et al. Optical coherence tomography. Science 1991; 254:1178-81; PMID:1957169; http://dx.doi.org/10.1126/science.1957169
2. Fujimoto JG, Brezinski ME, Tearney GJ, Boppart SA, Bouma B, Hee MR, Southern JF, Swanson EA. Optical biopsy and imaging using optical coherence tomography. Nat Med 1995; 1:970-2; PMID:7585229; http://dx.doi.org/10.1038/nm0995-970
3. Yaqoob Z, Wu J, McDowell EJ, Heng X, Yang C. Methods and application areas of endoscopic optical coherence tomography. J Biomed Opt 2006; 11:063001; PMID:17212523; http://dx.doi.org/10.1117/1.2400214
4. Liang CP, Chen CW, Desai J, Gullapalli R, Tang CM, Mezrich R, Chen Y. Endoscopic microscopy using optical coherence tomography. Current Medical Imaging Reviews 2012; 8:174-93; http://dx.doi.org/10.2174/157340512803759910
5. Choma M, Sarunic M, Yang C, Izatt J. Sensitivity advantage of swept source and Fourier domain optical coherence tomography. Opt Express 2003; 11:2183-9; PMID:19466106; http://dx.doi.org/10.1364/OE.11.002183
6. de Boer JF, Cense B, Park BH, Pierce MC, Tearney GJ, Bouma BE. Improved signal-to-noise ratio in spectral-domain compared with time-domain optical coherence tomography. Opt Lett 2003; 28:2067-9; PMID:14587817; http://dx.doi.org/10.1364/OL.28.002067
7. Leitgeb R, Hitzenberger C, Fercher A. Performance of fourier domain vs. time domain optical coherence tomography. Opt Express 2003; 11:889-94; PMID:19461802; http://dx.doi.org/10.1364/OE.11.000889
8. Fercher AF, Hitzenberger CK, Kamp G, Elzaiat SY. Measurement of Intraocular Distances by Backscattering Spectral Interferometry. Opt Commun 1995; 117:43-8; http://dx.doi.org/10.1016/0030-4018(95)00119-S
9. Wojtkowski M, Leitgeb R, Kowalczyk A, Bajraszewski T, Fercher AF. In vivo human retinal imaging by Fourier domain optical coherence tomography. J Biomed Opt 2002; 7:457-63; PMID:12175297; http://dx.doi.org/10.1117/1.1482379
10. Chinn SR, Swanson EA, Fujimoto JG. Optical coherence tomography using a frequency-tunable optical source. Opt Lett 1997; 22:340-2; PMID:18183195; http://dx.doi.org/10.1364/OL.22.000340
11. Golubovic B, Bouma BE, Tearney GJ, Fujimoto JG. Optical frequency-domain reflectometry using rapid wavelength tuning of a Cr4+:forsterite laser. Opt Lett 1997; 22:1704-6; PMID:18188341; http://dx.doi.org/10.1364/OL.22.001704
12. Yun S, Tearney G, de Boer J, Iftimia N, Bouma B. High-speed optical frequency-domain imaging. Opt Express 2003; 11:2953-63; PMID:19471415; http://dx.doi.org/10.1364/OE.11.002953
13. Adler DC, Chen Y, Huber R, Schmitt J, Connolly J, Fujimoto JG. Three-dimensional endomicroscopy using optical coherence tomography. Nat Photonics 2007; 1:709-16; http://dx.doi.org/10.1038/nphoton.2007.228
14. Vakoc BJ, Shishko M, Yun SH, Oh WY, Suter MJ, Desjardins AE, Evans JA, Nishioka NS, Tearney GJ, Bouma BE. Comprehensive esophageal microscopy by using optical frequency-domain imaging (with video). Gastrointest Endosc 2007; 65:898-905; PMID:17383652; http://dx.doi.org/10.1016/j.gie.2006.08.009
15. Zhou C, Adler DC, Becker L, Chen Y, Tsai TH, Figueiredo M, Schmitt JM, Fujimoto JG, Mashimo H. Effective treatment of chronic radiation proctitis using radiofrequency ablation. Therap Adv Gastroenterol 2009; 2:149-56; PMID:20593010; http://dx.doi.org/10.1177/1756283X08103341
16. Zhou C, Tsai TH, Lee HC, Kirtane T, Figueiredo M, Tao YK, Ahsen OO, Adler DC, Schmitt JM, Huang Q, et al. Characterization of buried glands before and after radiofrequency ablation by using 3-dimensional optical coherence tomography (with videos). Gastrointest Endosc 2012; 76:32-40; PMID:22482920; http://dx.doi.org/10.1016/j.gie.2012.02.003
17. Zysk AM, Nguyen FT, Oldenburg AL, Marks DL, Boppart SA. Optical coherence tomography: a review of clinical development from bench to bedside. J Biomed Opt 2007; 12:051403; PMID:17994864; http://dx.doi.org/10.1117/1.2793736
18. Tearney GJ, Brezinski ME, Bouma BE, Boppart SA, Pitris C, Southern JF, Fujimoto JG. In vivo endoscopic optical biopsy with optical coherence tomography. Science 1997; 276:2037-9; PMID:9197265; http://dx.doi.org/10.1126/science.276.5321.2037
19. Herz P, Chen Y, Aguirre A, Fujimoto J, Mashimo H, Schmitt J, Koski A, Goodnow J, Petersen C. Ultrahigh resolution optical biopsy with endoscopic optical coherence tomography. Opt Express 2004; 12:3532-42; PMID:19483882; http://dx.doi.org/10.1364/OPEX.12.003532
20. Boppart SA, Bouma BE, Pitris C, Tearney GJ, Fujimoto JG, Brezinski ME. Forward-imaging instruments for optical coherence tomography. Opt Lett 1997; 22:1618-20; PMID:18188315; http://dx.doi.org/10.1364/OL.22.001618
21. Hariri LP, Bonnema GT, Schmidt K, Winkler AM, Korde V, Hatch KD, Davis JR, Brewer MA, Barton JK. Laparoscopic optical coherence tomography imaging of human ovarian cancer. Gynecol Oncol 2009; 114:188-94; PMID:19481241; http://dx.doi.org/10.1016/j.ygyno.2009.05.014
22. Li X, Chudoba C, Ko T, Pitris C, Fujimoto JG. Imaging needle for optical coherence tomography. Opt Lett 2000; 25:1520-2; PMID:18066265; http://dx.doi.org/10.1364/OL.25.001520

23. Han S, Sarunic MV, Wu J, Humayun M, Yang C. Handheld forward-imaging needle endoscope for ophthalmic optical coherence tomography inspection. J Biomed Opt 2008; 13:020505; PMID:18465947; http://dx.doi.org/10.1117/1.2904664
24. Scolaro L, Lorenser D, McLaughlin RA, Quirk BC, Kirk RW, Sampson DD. High-sensitivity anastigmatic imaging needle for optical coherence tomography. Opt Lett 2012; 37:5247-9; PMID:23258067; http://dx.doi.org/10.1364/OL.37.005247
25. Kuo WC, Kim J, Shemonski ND, Chaney EJ, Spillman DR Jr., Boppart SA. Real-time three-dimensional optical coherence tomography image-guided core-needle biopsy system. Biomed Opt Express 2012; 3:1149-61; PMID:22741064; http://dx.doi.org/10.1364/BOE.3.001149
26. Liang CP, Wierwille J, Moreira T, Schwartzbauer G, Jafri MS, Tang CM, Chen Y. A forward-imaging needle-type OCT probe for image guided stereotactic procedures. Opt Express 2011; 19:26283-94; PMID:22274213; http://dx.doi.org/10.1364/OE.19.026283
27. Song C, Park DY, Gehlbach PL, Park SJ, Kang JU. Fiber-optic OCT sensor guided "SMART" micro-forceps for microsurgery. Biomed Opt Express 2013; 4:1045-50; PMID:23847730; http://dx.doi.org/10.1364/BOE.4.001045
28. Sergeev A, Gelikonov V, Gelikonov G, Feldchtein F, Kuranov R, Gladkova N, Shakhova N, Snopova L, Shakhov A, Kuznetzova I, et al. In vivo endoscopic OCT imaging of precancer and cancer states of human mucosa. Opt Express 1997; 1:432-40; PMID:19377567; http://dx.doi.org/10.1364/OE.1.000432
29. Pan Y, Xie H, Fedder GK. Endoscopic optical coherence tomography based on a microelectromechanical mirror. Opt Lett 2001; 26:1966-8; PMID:18059747; http://dx.doi.org/10.1364/OL.26.001966
30. Xie H, Pan Y, Fedder GK. Endoscopic optical coherence tomographic imaging with a CMOS-MEMS micromirror. Sens Actuators A Phys 2003; A103:237-41; http://dx.doi.org/10.1016/S0924-4247(02)00347-3
31. Pan Y, Li Z, Xie T, Chu CR. Hand-held arthroscopic optical coherence tomography for in vivo high-resolution imaging of articular cartilage. J Biomed Opt 2003; 8:648-54; PMID:14563203; http://dx.doi.org/10.1117/1.1609201
32. Jain A, Kopa A, Pan YT, Fedder GK, Xie HK. A two-axis electrothermal micromirror for endoscopic optical coherence tomography. IEEE J Sel Top Quantum Electron 2004; 10:636-42; http://dx.doi.org/10.1109/JSTQE.2004.829194
33. Tran PH, Mukai DS, Brenner M, Chen Z. In vivo endoscopic optical coherence tomography by use of a rotational microelectromechanical system probe. Opt Lett 2004; 29:1236-8; PMID:15209258; http://dx.doi.org/10.1364/OL.29.001236
34. Herz PR, Chen Y, Aguirre AD, Schneider K, Hsiung P, Fujimoto JG, Madden K, Schmitt J, Goodnow J, Petersen C. Micromotor endoscope catheter for in vivo, ultrahigh-resolution optical coherence tomography. Opt Lett 2004; 29:2261-3; PMID:15524374; http://dx.doi.org/10.1364/OL.29.002261
35. Liu X, Cobb MJ, Chen Y, Kimmey MB, Li X. Rapid-scanning forward-imaging miniature endoscope for real-time optical coherence tomography. Opt Lett 2004; 29:1763-5; PMID:15352362; http://dx.doi.org/10.1364/OL.29.001763
36. Tumlinson AR, Hariri LP, Utzinger U, Barton JK. Miniature endoscope for simultaneous optical coherence tomography and laser-induced fluorescence measurement. Appl Opt 2004; 43:113-21; PMID:14714651; http://dx.doi.org/10.1364/AO.43.000113
37. Yeow JTW, Yang VXD, Chahwan A, Gordon ML, Qi B, Vitkin IA, Wilson BC, Goldenberg AA. Micromachined 2-D scanner for 3-D optical coherence tomography. Sens Actuators A Phys 2005; 117:331-40; http://dx.doi.org/10.1016/j.sna.2004.06.021
38. Yang VXD, Mao YX, Munce N, Standish B, Kucharczyk W, Marcon NE, Wilson BC, Vitkin IA. Interstitial Doppler optical coherence tomography. Opt Lett 2005; 30:1791-3; PMID:16092347; http://dx.doi.org/10.1364/OL.30.001791
39. Xie T, Mukai D, Guo S, Brenner M, Chen Z. Fiber-optic-bundle-based optical coherence tomography. Opt Lett 2005; 30:1803-5; PMID:16092351; http://dx.doi.org/10.1364/OL.30.001803
40. Xie T, Guo S, Chen Z, Mukai D, Brenner M. GRIN lens rod based probe for endoscopic spectral domain optical coherence tomography with fast dynamic focus tracking. Opt Express 2006; 14:3238-46; PMID:19516465; http://dx.doi.org/10.1364/OE.14.003238
41. Böhringer HJ, Lankenau E, Rohde V, Hüttmann G, Giese A. Optical coherence tomography for experimental neuroendoscopy. Minim Invasive Neurosurg 2006; 49:269-75; PMID:17163339; http://dx.doi.org/10.1055/s-2006-954574
42. Wu J, Conry M, Gu C, Wang F, Yaqoob Z, Yang C. Paired-angle-rotation scanning optical coherence tomography forward-imaging probe. Opt Lett 2006; 31:1265-7; PMID:16642080; http://dx.doi.org/10.1364/OL.31.001265
43. Jung W, McCormick DT, Zhang J, Wang L, Tien NC, Chen ZP. Three-dimensional endoscopic optical coherence tomography by use of a two-axis microelectromechanical scanning mirror. Appl Phys Lett 2006; 88:163901
44. Fercher AF, Drexler W, Hitzenberger CK, Lasser T. Optical coherence tomography-principles and applications. Rep Prog Phys 2003; 66:239-303; http://dx.doi.org/10.1088/0034-4885/66/2/204
45. Fujimoto JG. Optical coherence tomography for ultrahigh resolution in vivo imaging. Nat Biotechnol 2003; 21:1361-7; PMID:14595364; http://dx.doi.org/10.1038/nbt892
46. Bouma BE, Tearney GJ. Clinical imaging with optical coherence tomography. Acad Radiol 2002; 9:942-53; PMID:12186444; http://dx.doi.org/10.1016/S1076-6332(03)80465-8
47. Walther J, Gaertner M, Cimalla P, Burkhardt A, Kirsten L, Meissner S, Koch E. Optical coherence tomography in biomedical research. Anal Bioanal Chem 2011; 400:2721-43; PMID:21562739; http://dx.doi.org/10.1007/s00216-011-5052-x
48. Drexler W, Fujimoto JG. State-of-the-art retinal optical coherence tomography. Prog Retin Eye Res 2008; 27:45-88; PMID:18036865; http://dx.doi.org/10.1016/j.preteyeres.2007.07.005
49. Brezinski ME, Tearney GJ, Bouma BE, Boppart SA, Hee MR, Swanson EA, Southern JF, Fujimoto JG. Imaging of coronary artery microstructure (in vitro) with optical coherence tomography. Am J Cardiol 1996; 77:92-3; PMID:8540467; http://dx.doi.org/10.1016/S0002-9149(97)89143-6
50. Fujimoto JG, Boppart SA, Tearney GJ, Bouma BE, Pitris C, Brezinski ME. High resolution in vivo intra-arterial imaging with optical coherence tomography. Heart 1999; 82:128-33; PMID:10409522
51. Jang IK, Tearney G, Bouma B. Visualization of tissue prolapse between coronary stent struts by optical coherence tomography: comparison with intravascular ultrasound. Circulation 2001; 104:2754; PMID:11723031; http://dx.doi.org/10.1161/hc4701.098069
52. Zysk AM, Nguyen FT, Oldenburg AL, Marks DL, Boppart SA. Optical coherence tomography: a review of clinical development from bench to bedside. J Biomed Opt 2007; 12:051403; PMID:17994864; http://dx.doi.org/10.1117/1.2793736
53. Izatt JA, Kulkarni MD, Wang H-W, Kobayashi K, Sivak MV Jr. Optical coherence tomography and microscopy in gastrointestinal tissues. IEEE J Sel Top Quantum Electron 1996; 2:1017-28; http://dx.doi.org/10.1109/2944.577331
54. Tearney GJ, Brezinski ME, Southern JF, Bouma BE, Boppart SA, Fujimoto JG. Optical biopsy in human gastrointestinal tissue using optical coherence tomography. Am J Gastroenterol 1997; 92:1800-4; PMID:9382040
55. Kobayashi K, Izatt JA, Kulkarni MD, Willis J, Sivak MV Jr. High-resolution cross-sectional imaging of the gastrointestinal tract using optical coherence tomography: preliminary results. Gastrointest Endosc 1998; 47:515-23; PMID:9647378; http://dx.doi.org/10.1016/S0016-5107(98)70254-8
56. Bouma BE, Tearney GJ, Compton CC, Nishioka NS. High-resolution imaging of the human esophagus and stomach in vivo using optical coherence tomography. Gastrointest Endosc 2000; 51:467-74; PMID:10744824; http://dx.doi.org/10.1016/S0016-5107(00)70449-4
57. Sivak MV Jr., Kobayashi K, Izatt JA, Rollins AM, Ung-Runyawee R, Chak A, Wong RC, Isenberg GA, Willis J. High-resolution endoscopic imaging of the GI tract using optical coherence tomography. Gastrointest Endosc 2000; 51:474-9; PMID:10744825; http://dx.doi.org/10.1016/S0016-5107(00)70450-0
58. Li XD, Boppart SA, Van Dam J, Mashimo H, Mutinga M, Drexler W, Klein M, Pitris C, Krinsky ML, Brezinski ME, et al. Optical coherence tomography: advanced technology for the endoscopic imaging of Barrett's esophagus. Endoscopy 2000; 32:921-30; PMID:11147939; http://dx.doi.org/10.1055/s-2000-9626
59. Jäckle S, Gladkova N, Feldchtein F, Terentieva A, Brand B, Gelikonov G, Gelikonov V, Sergeev A, Fritscher-Ravens A, Freund J, et al. In vivo endoscopic optical coherence tomography of the human gastrointestinal tract--toward optical biopsy. Endoscopy 2000; 32:743-9; PMID:11068832; http://dx.doi.org/10.1055/s-2000-7711
60. Zuccaro G, Gladkova N, Vargo J, Feldchtein F, Zagaynova E, Conwell D, Falk G, Goldblum J, Dumot J, Ponsky J, et al. Optical coherence tomography of the esophagus and proximal stomach in health and disease. Am J Gastroenterol 2001; 96:2633-9; PMID:11569687; http://dx.doi.org/10.1111/j.1572-0241.2001.04119.x
61. Poneros JM, Brand S, Bouma BE, Tearney GJ, Compton CC, Nishioka NS. Diagnosis of specialized intestinal metaplasia by optical coherence tomography. Gastroenterology 2001; 120:7-12; PMID:11208708; http://dx.doi.org/10.1053/gast.2001.20911
62. Poneros JM, Tearney GJ, Shiskov M, Kelsey PB, Lauwers GY, Nishioka NS, Bouma BE. Optical coherence tomography of the biliary tree during ERCP. Gastrointest Endosc 2002; 55:84-8; PMID:11756925; http://dx.doi.org/10.1067/mge.2002.120098
63. Shen B, Zuccaro G Jr., Gramlich TL, Gladkova N, Trolli P, Kareta M, Delaney CP, Connor JT, Lashner BA, Bevins CL, et al. In vivo colonoscopic optical coherence tomography for transmural inflammation in inflammatory bowel disease. Clin Gastroenterol Hepatol 2004; 2:1080-7; PMID:15625653; http://dx.doi.org/10.1016/S1542-3565(04)00621-4
64. Yang VX, Tang SJ, Gordon ML, Qi B, Gardiner G, Cirocco M, Kortan P, Haber GB, Kandel G, Vitkin IA, et al. Endoscopic Doppler optical coherence tomography in the human GI tract: initial experience. Gastrointest Endosc 2005; 61:879-90; PMID:15933695; http://dx.doi.org/10.1016/S0016-5107(05)00323-8

65. Isenberg G, Sivak MV Jr., Chak A, Wong RCK, Willis JE, Wolf B, Rowland DY, Das A, Rollins A. Accuracy of endoscopic optical coherence tomography in the detection of dysplasia in Barrett's esophagus: a prospective, double-blinded study. Gastrointest Endosc 2005; 62:825-31; PMID:16301020; http://dx.doi.org/10.1016/j.gie.2005.07.048
66. Evans JA, Poneros JM, Bouma BE, Bressner J, Halpern EF, Shishkov M, Lauwers GY, Mino-Kenudson M, Nishioka NS, Tearney GJ. Optical coherence tomography to identify intramucosal carcinoma and high-grade dysplasia in Barrett's esophagus. Clin Gastroenterol Hepatol 2006; 4:38-43; PMID:16431303; http://dx.doi.org/10.1016/S1542-3565(05)00746-9
67. Chen Y, Aguirre AD, Hsiung PL, Desai S, Herz PR, Pedrosa M, Huang Q, Figueiredo M, Huang SW, Koski A, et al. Ultrahigh resolution optical coherence tomography of Barrett's esophagus: preliminary descriptive clinical study correlating images with histology. Endoscopy 2007; 39:599-605; PMID:17611914; http://dx.doi.org/10.1055/s-2007-966648
68. Welzel J, Lankenau E, Birngruber R, Engelhardt R. Optical coherence tomography of the human skin. J Am Acad Dermatol 1997; 37:958-63; PMID:9418764; http://dx.doi.org/10.1016/S0190-9622(97)70072-0
69. Welzel J, Lankenau E, Birngruber R, Engelhardt R. Optical coherence tomography of the skin. Curr Probl Dermatol 1998; 26:27-37; PMID:9597313; http://dx.doi.org/10.1159/000060573
70. Welzel J, Reinhardt C, Lankenau E, Winter C, Wolff HH. Changes in function and morphology of normal human skin: evaluation using optical coherence tomography. Br J Dermatol 2004; 150:220-5; PMID:14996091; http://dx.doi.org/10.1111/j.1365-2133.2004.05810.x
71. Otis LL, Everett MJ, Sathyam US, Colston BW Jr. Optical coherence tomography: a new imaging technology for dentistry. J Am Dent Assoc 2000; 131:511-4; PMID:10770016; http://dx.doi.org/10.14219/jada.archive.2000.0210
72. Otis LL, al-Sadhan RI, Meiers J, Redford-Badwal D. Identification of occlusal sealants using optical coherence tomography. J Clin Dent 2003; 14:7-10; PMID:12619263
73. de Melo LS, de Araujo RE, Freitas AZ, Zezell D, Vieira ND, Girkin J, Hall A, Carvalho MT, Gomes AS. Evaluation of enamel dental restoration interface by optical coherence tomography. J Biomed Opt 2005; 10:064027; PMID:16409092; http://dx.doi.org/10.1117/1.2141617
74. Tearney GJ, Brezinski ME, Southern JF, Bouma BE, Boppart SA, Fujimoto JG. Optical biopsy in human urologic tissue using optical coherence tomography. J Urol 1997; 157:1915-9; PMID:9112562; http://dx.doi.org/10.1016/S0022-5347(01)64900-0
75. D'Amico AV, Weinstein M, Li X, Richie JP, Fujimoto J. Optical coherence tomography as a method for identifying benign and malignant microscopic structures in the prostate gland. Urology 2000; 55:783-7; PMID:10792101; http://dx.doi.org/10.1016/S0090-4295(00)00475-1
76. Zagaynova EV, Streltsova OS, Gladkova ND, Snopova LB, Gelikonov GV, Feldchtein FI, Morozov A. In vivo optical coherence tomography feasibility for bladder disease. J Urol 2002; 167:1492-6; PMID:11832776; http://dx.doi.org/10.1016/S0022-5347(05)65351-7
77. Manyak MJ, Gladkova ND, Makari JH, Schwartz AM, Zagaynova EV, Zolfaghari L, Zara JM, Iksanov R, Feldchtein FI. Evaluation of superficial bladder transitional-cell carcinoma by optical coherence tomography. J Endourol 2005; 19:570-4; PMID:15989448; http://dx.doi.org/10.1089/end.2005.19.570
78. Pitris C, Goodman A, Boppart SA, Libus JJ, Fujimoto JG, Brezinski ME. High-resolution imaging of gynecologic neoplasms using optical coherence tomography. Obstet Gynecol 1999; 93:135-9; PMID:9916971
79. Boppart SA, Goodman A, Libus J, Pitris C, Jesser CA, Brezinski ME, Fujimoto JG. High resolution imaging of endometriosis and ovarian carcinoma with optical coherence tomography: feasibility for laparoscopic-based imaging. Br J Obstet Gynaecol 1999; 106:1071-7; PMID:10519434; http://dx.doi.org/10.1111/j.1471-0528.1999.tb08116.x
80. Brewer MA, Utzinger U, Barton JK, Hoying JB, Kirkpatrick ND, Brands WR, Davis JR, Hunt K, Stevens SJ, Gmitro AF. Imaging of the ovary. Technol Cancer Res Treat 2004; 3:617-27; PMID:15560720
81. Boppart SA, Luo W, Marks DL, Singletary KW. Optical coherence tomography: feasibility for basic research and image-guided surgery of breast cancer. Breast Cancer Res Treat 2004; 84:85-97; PMID:14999139; http://dx.doi.org/10.1023/B:BREA.0000018401.13609.54
82. Hsiung PL, Phatak DR, Chen Y, Aguirre AD, Fujimoto JG, Connolly JL. Benign and malignant lesions in the human breast depicted with ultrahigh resolution and three-dimensional optical coherence tomography. Radiology 2007; 244:865-74; PMID:17630358; http://dx.doi.org/10.1148/radiol.2443061536
83. Goldberg BD, Iftimia NV, Bressner JE, Pitman MB, Halpern E, Bouma BE, Tearney GJ. Automated algorithm for differentiation of human breast tissue using low coherence interferometry for fine needle aspiration biopsy guidance. J Biomed Opt 2008; 13:014014; PMID:18315372; http://dx.doi.org/10.1117/1.2837433
84. Nguyen FT, Zysk AM, Chaney EJ, Kotynek JG, Oliphant UJ, Bellafiore FJ, Rowland KM, Johnson PA, Boppart SA. Intraoperative evaluation of breast tumor margins with optical coherence tomography. Cancer Res 2009; 69:8790-6; PMID:19910294; http://dx.doi.org/10.1158/0008-5472.CAN-08-4340
85. Zhou C, Cohen DW, Wang Y, Lee HC, Mondelblatt AE, Tsai TH, Aguirre AD, Fujimoto JG, Connolly JL. Integrated optical coherence tomography and microscopy for ex vivo multiscale evaluation of human breast tissues. Cancer Res 2010; 70:10071-9; PMID:21056988; http://dx.doi.org/10.1158/0008-5472.CAN-10-2968
86. Pan Y, Lavelle JP, Bastacky SI, Meyers S, Pirtskhalaishvili G, Zeidel ML, Farkas DL. Detection of tumorigenesis in rat bladders with optical coherence tomography. Med Phys 2001; 28:2432-40; PMID:11797946; http://dx.doi.org/10.1118/1.1418726
87. Yuan Z, Wang Z, Pan R, Liu J, Cohen H, Pan Y. High-resolution imaging diagnosis and staging of bladder cancer: comparison between optical coherence tomography and high-frequency ultrasound. J Biomed Opt 2008; 13:054007; PMID:19021387; http://dx.doi.org/10.1117/1.2978059
88. Lingley-Papadopoulos CA, Loew MH, Manyak MJ, Zara JM. Computer recognition of cancer in the urinary bladder using optical coherence tomography and texture analysis. J Biomed Opt 2008; 13:024003; PMID:18465966; http://dx.doi.org/10.1117/1.2904987
89. Goh AC, Tresser NJ, Shen SS, Lerner SP. Optical coherence tomography as an adjunct to white light cystoscopy for intravesical real-time imaging and staging of bladder cancer. Urology 2008; 72:133-7; PMID:18598789; http://dx.doi.org/10.1016/j.urology.2008.02.002
90. Boppart SA, Brezinski ME, Pitris C, Fujimoto JG. Optical coherence tomography for neurosurgical imaging of human intracortical melanoma. Neurosurgery 1998; 43:834-41; PMID:9766311; http://dx.doi.org/10.1097/00006123-199810000-00068
91. Bizheva K, Unterhuber A, Hermann B, Povazay B, Sattmann H, Fercher AF, Drexler W, Preusser M, Budka H, Stingl A, et al. Imaging ex vivo healthy and pathological human brain tissue with ultra-high-resolution optical coherence tomography. J Biomed Opt 2005; 10:11006-1; PMID:15847572; http://dx.doi.org/10.1117/1.1851513
92. Böhringer HJ, Boller D, Leppert J, Knopp U, Lankenau E, Reusche E, Hüttmann G, Giese A. Time-domain and spectral-domain optical coherence tomography in the analysis of brain tumor tissue. Lasers Surg Med 2006; 38:588-97; PMID:16736504; http://dx.doi.org/10.1002/lsm.20353
93. Qi X, Sivak MV, Isenberg G, Willis JE, Rollins AM. Computer-aided diagnosis of dysplasia in Barrett's esophagus using endoscopic optical coherence tomography. J Biomed Opt 2006; 11:044010; PMID:16965167; http://dx.doi.org/10.1117/1.2337314
94. Testoni PA, Mangiavillano B. Optical coherence tomography in detection of dysplasia and cancer of the gastrointestinal tract and bilio-pancreatic ductal system. World J Gastroenterol 2008; 14:6444-52; PMID:19030194; http://dx.doi.org/10.3748/wjg.14.6444
95. Lam S, Standish B, Baldwin C, McWilliams A, leRiche J, Gazdar A, Vitkin AI, Yang V, Ikeda N, MacAulay C. In vivo optical coherence tomography imaging of preinvasive bronchial lesions. Clin Cancer Res 2008; 14:2006-11; PMID:18381938; http://dx.doi.org/10.1158/1078-0432.CCR-07-4418
96. Escobar PF, Belinson JL, White A, Shakhova NM, Feldchtein FI, Kareta MV, Gladkova ND. Diagnostic efficacy of optical coherence tomography in the management of preinvasive and invasive cancer of uterine cervix and vulva. Int J Gynecol Cancer 2004; 14:470-4; PMID:15228420; http://dx.doi.org/10.1111/j.1048-891x.2004.14307.x
97. Escobar PF, Rojas-Espaillat L, Tisci S, Enerson C, Brainard J, Smith J, Tresser NJ, Feldchtein FI, Rojas LB, Belinson JL. Optical coherence tomography as a diagnostic aid to visual inspection and colposcopy for preinvasive and invasive cancer of the uterine cervix. Int J Gynecol Cancer 2006; 16:1815-22; PMID:17009977; http://dx.doi.org/10.1111/j.1525-1438.2006.00665.x
98. Mogensen M, Joergensen TM, Nürnberg BM, Morsy HA, Thomsen JB, Thrane L, Jemec GBE. Assessment of optical coherence tomography imaging in the diagnosis of non-melanoma skin cancer and benign lesions versus normal skin: observer-blinded evaluation by dermatologists and pathologists. Dermatol Surg 2009; 35:965-72; PMID:19397661; http://dx.doi.org/10.1111/j.1524-4725.2009.01164.x
99. Shakhov AV, Terentjeva AB, Kamensky VA, Snopova LB, Gelikonov VM, Feldchtein FI, Sergeev AM. Optical coherence tomography monitoring for laser surgery of laryngeal carcinoma. J Surg Oncol 2001; 77:253-8; PMID:11473374; http://dx.doi.org/10.1002/jso.1105
100. Armstrong WB, Ridgway JM, Vokes DE, Guo S, Perez J, Jackson RP, Gu M, Su J, Crumley RL, Shibuya TY, et al. Optical coherence tomography of laryngeal cancer. Laryngoscope 2006; 116:1107-13; PMID:16826043; http://dx.doi.org/10.1097/01.mlg.0000217539.27432.5a
101. Jung WG, Zhang J, Chung JR, Wilder-Smith P, Brenner M, Nelson JS, Chen ZP. Advances in oral cancer detection using optical coherence tomography. IEEE J Sel Top Quantum Electron 2005; 11:811-7; http://dx.doi.org/10.1109/JSTQE.2005.857678

102. Tsai MT, Lee HC, Lu CW, Wang YM, Lee CK, Yang CC, Chiang CP. Delineation of an oral cancer lesion with swept-source optical coherence tomography. J Biomed Opt 2008; 13:044012; PMID:19021340; http://dx.doi.org/10.1117/1.2960632
103. Motreff P, Souteyrand G. Optical coherence tomography to diagnose under-expansion of a drug-eluting stent. JACC Cardiovasc Imaging 2009; 2:245-6, author reply 246; PMID:19356563; http://dx.doi.org/10.1016/j.jcmg.2008.11.008
104. Messing EM, Catalona W. Urothelial tumors of the urinary tract. In: Walsh PC, Retik A, WVaughan ED, Wein AJ, eds. Campbell's Urology. St Louis: WB Saunders Company, 1998:2327-10.
105. Jesser CA, Boppart SA, Pitris C, Stamper DL, Nielsen GP, Brezinski ME, Fujimoto JG. High resolution imaging of transitional cell carcinoma with optical coherence tomography: feasibility for the evaluation of bladder pathology. Br J Radiol 1999; 72:1170-6; PMID:10703474
106. Hermes B, Spöler F, Naami A, Bornemann J, Först M, Grosse J, Jakse G, Knüchel R. Visualization of the basement membrane zone of the bladder by optical coherence tomography: feasibility of noninvasive evaluation of tumor invasion. Urology 2008; 72:677-81; PMID:18455778; http://dx.doi.org/10.1016/j.urology.2008.02.062
107. Ren H, Waltzer WC, Bhalla R, Liu J, Yuan Z, Lee CS, Darras F, Schulsinger D, Adler HL, Kim J, et al. Diagnosis of bladder cancer with microelectromechanical systems-based cystoscopic optical coherence tomography. Urology 2009; 74:1351-7; PMID:19660795; http://dx.doi.org/10.1016/j.urology.2009.04.090
108. Zagaynova E, Gladkova N, Shakhova N, Gelikonov G, Gelikonov V. Endoscopic OCT with forward-looking probe: clinical studies in urology and gastroenterology. J Biophotonics 2008; 1:114-28; PMID:19343643; http://dx.doi.org/10.1002/jbio.200710017
109. Wang Z, Lee CS, Waltzer WC, Liu J, Xie H, Yuan Z, Pan Y. In vivo bladder imaging with microelectromechanical-systems-based endoscopic spectral domain optical coherence tomography. J Biomed Opt 2007; 12:034009; PMID:17614717; http://dx.doi.org/10.1117/1.2749744
110. Cauberg Evelyne CC, de la Rosette JJ, de Reijke TM. Emerging optical techniques in advanced cystoscopy for bladder cancer diagnosis: A review of the current literature. Indian J Urol 2011; 27:245-51; PMID:21814317; http://dx.doi.org/10.4103/0970-1591.82845
111. Leyh H, Marberger M, Conort P, Sternberg C, Pansadoro V, Pagano F, Bassi P, Boccon-Gibod L, Ravery V, Treiber U, et al. Comparison of the BTA stat test with voided urine cytology and bladder wash cytology in the diagnosis and monitoring of bladder cancer. Eur Urol 1999; 35:52-6; PMID:9933795; http://dx.doi.org/10.1159/000019819
112. Kriegmair M, Baumgartner R, Knüchel R, Stepp H, Hofstädter F, Hofstetter A. Detection of early bladder cancer by 5-aminolevulinic acid induced porphyrin fluorescence. J Urol 1996; 155:105-9, discussion 109-10; PMID:7490803; http://dx.doi.org/10.1016/S0022-5347(01)66559-5
113. Ikeda M, Matsumoto K, Choi D, Nishi M, Fujita T, Ohbayashi K, Shimizu K, Iwamura M. The impact of real-time 3d imaging by ultra-high speed optical coherence tomography in urothelial carcinoma. BMC Urol 2013; 13:65; PMID:24289823; http://dx.doi.org/10.1186/1471-2490-13-65
114. Liu JJ, Droller MJ, Liao JC. New optical imaging technologies for bladder cancer: considerations and perspectives. J Urol 2012; 188:361-8; PMID:22698620; http://dx.doi.org/10.1016/j.juro.2012.03.127
115. Pan YT, Xie TQ, Du CW, Bastacky S, Meyers S, Zeidel ML. Enhancing early bladder cancer detection with fluorescence-guided endoscopic optical coherence tomography. Opt Lett 2003; 28:2485-7; PMID:14690122; http://dx.doi.org/10.1364/OL.28.002485
116. El-Hakim A, Weiss GH, Lee BR, Smith AD. Correlation of ureteroscopic appearance with histologic grade of upper tract transitional cell carcinoma. Urology 2004; 63:647-50, discussion 650; PMID:15072870; http://dx.doi.org/10.1016/j.urology.2003.10.076
117. Mueller-Lisse UL, Meissner OA, Babaryka G, Bauer M, Eibel R, Stief CG, Reiser MF, Mueller-Lisse UG. Catheter-based intraluminal optical coherence tomography (OCT) of the ureter: ex-vivo correlation with histology in porcine specimens. Eur Radiol 2006; 16:2259-64; PMID:16572332; http://dx.doi.org/10.1007/s00330-006-0191-8
118. Wang H, Kang W, Zhu H, MacLennan G, Rollins AM. Three-dimensional imaging of ureter with endoscopic optical coherence tomography. Urology 2011; 77:1254-8; PMID:21256548; http://dx.doi.org/10.1016/j.urology.2010.11.044
119. Bus MT, Muller BG, de Bruin DM, Faber DJ, Kamphuis GM, van Leeuwen TG, de Reijke TM, de la Rosette JJ. Volumetric in vivo visualization of upper urinary tract tumors using optical coherence tomography: a pilot study. J Urol 2013; 190:2236-42; PMID:23954585; http://dx.doi.org/10.1016/j.juro.2013.08.006
120. Barwari K, de Bruin DM, Cauberg EC, Faber DJ, van Leeuwen TG, Wijkstra H, de la Rosette J, Laguna MP. Advanced diagnostics in renal mass using optical coherence tomography: a preliminary report. J Endourol 2011; 25:311-5; PMID:21235359; http://dx.doi.org/10.1089/end.2010.0408
121. Barwari K, de Bruin DM, Faber DJ, van Leeuwen TG, de la Rosette JJ, Laguna MP. Differentiation between normal renal tissue and renal tumours using functional optical coherence tomography: a phase I in vivo human study. BJU Int 2012; 110(8 Pt B):E415-20; PMID:22574685; http://dx.doi.org/10.1111/j.1464-410X.2012.11197.x
122. Linehan JA, Bracamonte ER, Hariri LP, Sokoloff MH, Rice PS, Barton JK, Nguyen MM. Feasibility of optical coherence tomography imaging to characterize renal neoplasms: limitations in resolution and depth of penetration. BJU Int 2011; 108:1820-4; PMID:21592299; http://dx.doi.org/10.1111/j.1464-410X.2011.10282.x
123. Li Q, Onozato ML, Andrews PM, Chen CW, Paek A, Naphas R, Yuan S, Jiang J, Cable A, Chen Y. Automated quantification of microstructural dimensions of the human kidney using optical coherence tomography (OCT). Opt Express 2009; 17:16000-16; PMID:19724599; http://dx.doi.org/10.1364/OE.17.016000
124. Onozato ML, Andrews PM, Li Q, Jiang J, Cable A, Chen Y. Optical coherence tomography of human kidney. J Urol 2010; 183:2090-4; PMID:20303512; http://dx.doi.org/10.1016/j.juro.2009.12.091
125. Wierwille J, Andrews PM, Onozato ML, Jiang J, Cable A, Chen Y. In vivo, label-free, three-dimensional quantitative imaging of kidney microcirculation using Doppler optical coherence tomography. Lab Invest 2011; 91:1596-604; PMID:21808233; http://dx.doi.org/10.1038/labinvest.2011.112
126. Andrews PM, Wang HW, Wierwille J, Gong W, Verbesey J, Cooper M, Chen Y. Optical coherence tomography of the living human kidney. Journal of Innovative Optical Health Sciences 2014; 7:1350064; http://dx.doi.org/10.1142/S1793545813500648
127. Frank I, Blute ML, Cheville JC, Lohse CM, Weaver AL, Zincke H. Solid renal tumors: an analysis of pathological features related to tumor size. J Urol 2003; 170:2217-20; PMID:14634382; http://dx.doi.org/10.1097/01.ju.0000095475.12515.5e
128. Campbell SC, Novick AC, Belldegrun A, Blute ML, Chow GK, Derweesh IH, Faraday MM, Kaouk JH, Leveillee RJ, Matin SF, et al.; Practice Guidelines Committee of the American Urological Association. Guideline for management of the clinical T1 renal mass. J Urol 2009; 182:1271-9; PMID:19683266; http://dx.doi.org/10.1016/j.juro.2009.07.004
129. Perico N, Cattaneo D, Sayegh MH, Remuzzi G. Delayed graft function in kidney transplantation. Lancet 2004; 364:1814-27; PMID:15541456; http://dx.doi.org/10.1016/S0140-6736(04)17406-0
130. Sanfilippo F, Vaughn WK, Spees EK, Lucas BA. The detrimental effects of delayed graft function in cadaver donor renal transplantation. Transplantation 1984; 38:643-8; PMID:6390827; http://dx.doi.org/10.1097/00007890-198412000-00019
131. Klein T, Wieser W, Reznicek L, Neubauer A, Kampik A, Huber R. Multi-MHz retinal OCT. Biomed Opt Express 2013; 4:1890-908; PMID:24156052; http://dx.doi.org/10.1364/BOE.4.001890
132. Jayaraman V, Cole GD, Robertson M, Uddin A, Cable A. High-sweep-rate 1310 nm MEMS-VCSEL with 150 nm continuous tuning range. Electron Lett 2012; 48:867-9; PMID:23976788; http://dx.doi.org/10.1049/el.2012.1552
133. Tsai TH, Potsaid B, Tao YK, Jayaraman V, Jiang J, Heim PJ, Kraus MF, Zhou C, Hornegger J, Mashimo H, et al. Ultrahigh speed endoscopic optical coherence tomography using micromotor imaging catheter and VCSEL technology. Biomed Opt Express 2013; 4:1119-32; PMID:23847737; http://dx.doi.org/10.1364/BOE.4.001119
134. Bus MT, Muller BG, de Bruin DM, Faber DJ, Kamphuis GM, van Leeuwen TG, de Reijke TM, de la Rosette JJ. Volumetric in vivo visualization of upper urinary tract tumors using optical coherence tomography: a pilot study. J Urol 2013; 190:2236-42; PMID:23954585; http://dx.doi.org/10.1016/j.juro.2013.08.006
135. Barwari K, de Bruin DM, Faber DJ, van Leeuwen TG, de la Rosette JJ, Laguna MP. Differentiation between normal renal tissue and renal tumours using functional optical coherence tomography: a phase I in vivo human study. BJU Int 2012; 110(8 Pt B):E415-20; PMID:22574685; http://dx.doi.org/10.1111/j.1464-410X.2012.11197.x